forward and backward directions, so that E-CARS and F-CARS are equal in intensity. By increasing L ($L > \lambda_p$), the forward signal starts to be stronger than the epi-detected signal because constructive interference is in the forward direction. As can be seen by eq. (9) the F-CARS signal intensity grows as L^2. On the contrary the epi-detected radiation is not phase-matched because in the backward direction $\Delta k = 2k_{aS} = 4\pi \frac{n_{aS}}{\lambda_{aS}}$, the direction of k_{aS} is reversed. As can be easily seen, the intensity of the E-CARS is proportional to $\lambda_{aS} \sin^2(2\pi n_{aS} L/\lambda_{aS})$ and oscillates as a function of L with a spatial period equal to half the CARS wavelength in the medium.

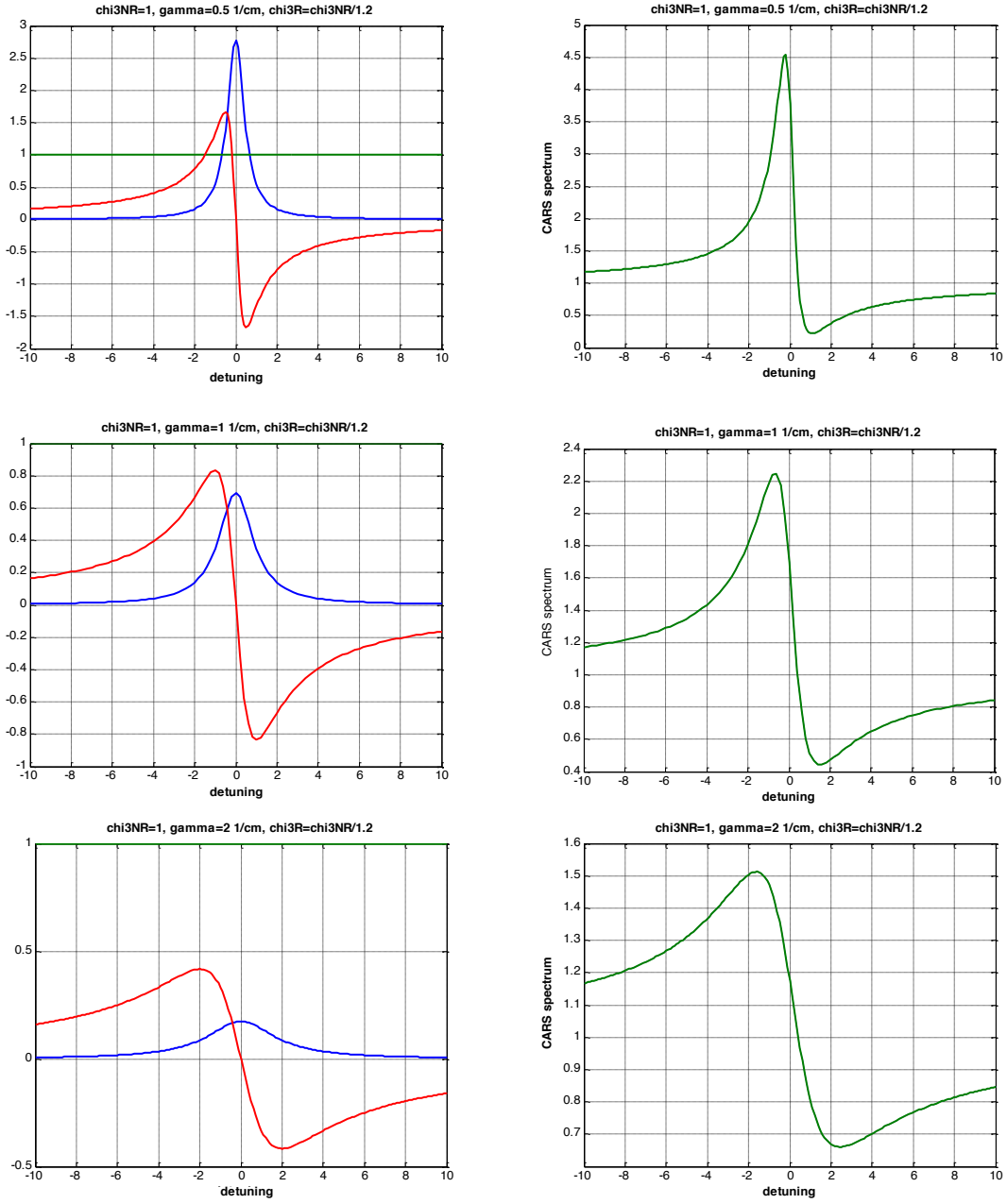

Fig. 2.2 Calculated third order nonlinear susceptibilities for different linewidths Γ_R. Figures on the left: $\left|\chi_{NR}^{(3)}\right|^2$ (green line), $\Re\left(\chi_R^{(3)}\right)$ (red curve), $\Im\left(\chi_R^{(3)}\right)$ (blue curve). Figures on the right: resulting CARS spectrum $\left|\chi_{1111}^{(3)}\right|^2$ First row: Γ_R=0.5 cm^{-1}. Second row: Γ_R=1.0 cm^{-1}. Third row: Γ_R=1.5 cm^{-1}.

It must be noted that the approach taken here is oversimplified and can be used only to explain the basic features of the radiation generated by the CARS process. In practical situations typical of CARS microscopy, the CARS interaction is obtained using tightly focused beams instead of plane waves, which generally in real experiments interact in the focal volume of a high NA microscope objective. A rigorous treatment taking into account local generation of CARS signals in the interaction volume and their coherent addition in the observation direction requires much more complex mathematics and can be found in [7] .

Coherent build up is an important feature of CARS signals. In the case of complex objects the spatial distribution of intensity may vary depending on the shape and size of the volume occupied by the non-linear material. To this respect, it is very instructive to report here the results of a numerical simulation carried out using the complete model where the CARS radiation generated by two tightly focussed excitation beams on a spherical sample is computed in the forward (F-CARS) and backward directions (E-CARS) as a function of the diameter *D* of the sample [8].

The results of the numerical simulation are shown in Fig. 2.3 (a) where the calculated E-CARS and F-CARS signals are plotted as a function of D/λ_p. The F-CARS signal starts to increase quasi-quadratically with *D* (similar to the plane wave case) and then becomes saturated when *D* exceeds the longitudinal dimension of the focal excitation volume, i.e., full width at half maximum (FWHM) 1.2 µm for the conditions assumed in the calculation. The E-CARS signal, however, appears only for small spheres and exhibits several maxima, with the highest one at $\sim 0.65\lambda_p$, and a periodicity close to that under the plane wave condition, that is $\sim(\lambda_{aS}/2n)$. The E-CARS signal intensity is negligible for large *D*, which resembles the case of focusing into an isotropic bulk medium. Please note that the curve of F-CARS has been compressed in order to show both calculated signal on the same vertical scale. Fig. 2.3 (b) shows the ratio of E-CARS and F-CARS as a function of *D*.

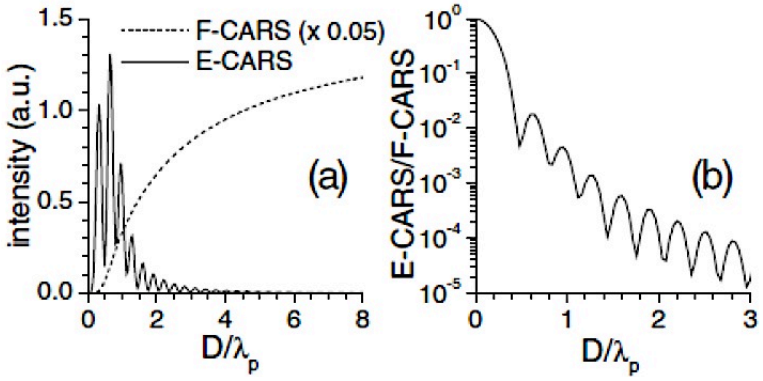

Fig. 2.3 Calculated F-CARS and E-CARS signals produced by a spherical sample. F-CARS and E-CARS as a function of the diameter the scatterer (a); the ratio of the two (b) (from [8])

Figure 2.3 clearly shows that E-CARS is not suited for observation of homogeneous samples, whereas it works very well when fine details of a structure are to be resolved. In the last case it should also be noted that when small scatterers diluted in a solvent or in a substrate are to be observed the contribution of the background of the solvent/substrate to E-CARS is negligible, because the solvent/substrate usually is homogeneous. This is an important advantage offered by epi-detection of CARS signals. Moreover for opaque samples E-CARS technique could detect stronger signal than those obtained using F-CARS technique.

Basic of two-photon excitation fluorescence (TPEF) microscopy

Two-photon excitation fluorescence microscopy was realized for the first time in 1990 by Denk et al. [9] using a physical principle predicted by Maria Göppert-Mayer in 1931, where an atom or a molecule could absorb two photons simultaneously in the same quantum event [10]. The spread of biological imaging using two-photon fluorescence microscopy is constantly increased, mainly thanks to the ability to excite UV-absorbing dyes with red or near-infrared light, reducing the damages on the samples due to the use of UV light. Moreover since the fluorescence intensity depends quadratically to the excitation power, the probability of a two-photon absorption is confined highly in the focal volume of the objective, guaranteeing a reduction of background fluorescence and an high confocal level without using any confocal pinhole [9]. Using infrared light it is also possible to penetrate deeper in tissue with respect to traditional fluorescence confocal microscopy making this technique particularly suitable for tissue engineering studies.

Two-photon excitation phenomena is based on the principle that an atom or a molecule can absorb two photons less energetic than that needed in one photon excitation (1PE), in the same quantum event. Subsequently the excited matter can emit a photon with a higher energy than those relative to the two absorbed ones. In this process the two exciting photons energy sum must be at least the one needed to drive the molecule or the atom in the excited state.

$$\frac{1}{\lambda_{1PE}} \leq \left(\frac{1}{\lambda_A} + \frac{1}{\lambda_B}\right) \tag{15}$$

In the equation (15) is depicted the relation between the expected one photon excitation wavelength λ_{1PE} and the two wavelengths λ_A and λ_B related to the excited photons. In many cases in order to simplify the experimental set-up, the two exciting photons have the same wavelength using a single excitation source.

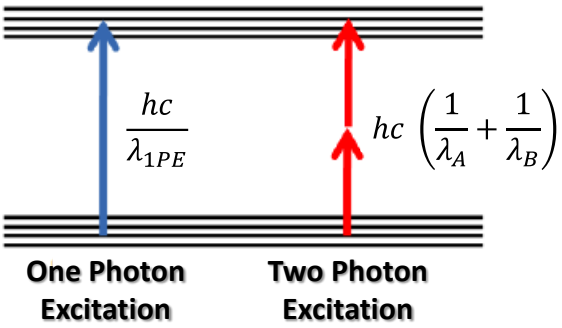

Fig. 2.4 Energy diagram of the two excitation processes.

The probability that an atom or a molecule absorbs two incident photons is proportional to the probability to find in the same molecular volume two photons when the matter is driven in an excited virtual state. This leads to the determination of a two-photon absorption cross-section δ_{TPE} that can be defined using the following formula according to Xu et al [11]:

$$\delta_{TPE} \approx \sum_m \delta_{fm}\delta_{mi}\tau_m \tag{16}$$

Where δ_{fm} and δ_{mi} are the single photon absorption cross sections for transition *to and from* an intermediate level *m* and τ_m is its lifetime (about 10^{-18}s [12]). The number of photons absorbed per second n_a by TPE is given thus by:

$$n_a = \delta_{TPE} I^2 \tag{17}$$

Where δ_{TPE} is the two-photon absorption cross-section measured as $cm^4 \cdot s \cdot photon^{-1}$ (expressed also in terms of the GM (Göppert-Mayer) units, where 1 GM = $10^{-50} \cdot cm^4 \cdot s \cdot photon^{-1}$) and *I* is the intensity expressed in terms of $photon \cdot cm^{-2} \cdot s^{-1}$. Since two photons are absorbed during the excitation of the fluorophore, the probability for fluorescent emission from the fluorophores increases quadratically with the excitation intensity. Therefore, when the Gaussian laser beam is focused on a sample the two-photon fluorescence intensity along the optical axis increases to the focus and then decreases raised at the fourth power [12].

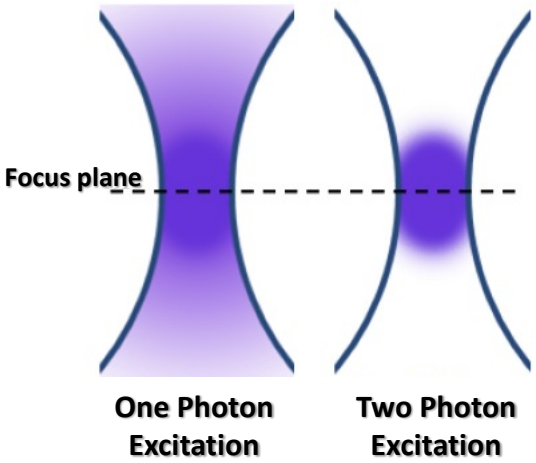

Fig. 2.5 Scratch of the fluorescence intensity distribution along the focused beam for the two excitation processes.

In this way the actual excitation is restricted to the tiny focal volume, resulting in a high degree of rejection of out-of-focus objects. This localization of excitation determines a high confocal level allowing a 3D optical sectioning of the sample limited only by the objective depth of focus. The use of pulsed light source is considered to be advantageous [9], since high peak power of pulses can give a large number of photons with a low average power avoiding possible sample photodamaging. Moreover the use of CW laser is limited due to enhanced optical tweezing effects that can affect imaging experiments [13]. Using pulsed laser source the number of absorbed photon per fluorophore per pulse depends according Denk et al. [9] by:

$$n_a \approx \frac{p_0^2 \delta_{TPE}}{\tau_p f_p^2} \left(\frac{NA^2}{2\hbar c \lambda}\right)^2 \tag{18}$$

Where p_0 is the average power of the laser, τ_p the pulse duration, f_p the repetition rate and NA the numerical aperture of the objective. It is quite easy to observe that the efficiency of the process can be in general increased reducing the pulse duration and the repetition rate and increasing the average laser power. If a rectangular temporal pulse shape is assumed according to Hänninen et al [13], the intensity of the TPEF signal $I_{f,pulsed}$ is given by:

$$I_{f,pulsed} \propto \frac{c p_0^2 \Delta t}{\tau_p f_p} \tag{19}$$

Where *c* denotes the constants associated with the optical system and Δt is the exposure time. Taking constant the exposure time and the average laser power, if 5 ps pulses are compared with 220 fs pulses,

the fluorescence intensity ratio obtained could be around 20 and around 11000 when CW laser is compared with 220 fs pulses Hänninen et al [13].

A prolongation of a pulse of a factor α could be fully compensated by increasing the average power p_0 by $\sqrt{\alpha}$, this compensation can be limited by the rise of heating and trapping effect [14]. Water heating can be however ruled out as a limiting factor of TPEF microscopy [15, 16].

Basic of second harmonic generation microscopy

Second harmonic generation was reported in the early 60s by Franken [17] and deeply demonstrated by Kleinman in crystalline quartz [18]. Since that time SHG was exploited in laser technology to double the output frequency of pulsed lasers. Later, Bloembergen discovered SHG from interfaces [19] and his work pushed this spectroscopy technique as standard to characterize surfaces and interfaces.

In 1974, Hellwarth was the first to implement SHG as an optical microscopy technique in order to image the crystal structure of polycrystalline ZnSe [20].

First biological SHG imaging experiments were in 1986 by Freund et al. [21] where it was studied the polar structure of rat tail connective tissue.

Campagnola in 2002 demonstrated the use of SHG microscopy technique to image successfully with 3D high spatial resolution endogenous structural proteins in biological tissues such as collagen, acto-myosin, and tubulin [22].

Second harmonic generation is a second order non-linear optical process that is generated in those particular materials that have non-centrosymmetric structures. In this case due to nonlinearity of the second order susceptibility $\chi^{(2)}$, the excitation pump signal wave generates a nonlinear polarization wave, which oscillates with twice the fundamental frequency. This nonlinear polarization wave radiates an electromagnetic field with this doubled frequency, allowing two photons with equal frequency to be absorbed and a photon with a doubled energy (and frequency) to be elastically emitted.

The intensity of the SHG signal depends by the second order susceptibility of the material $\chi^{(2)}$ and a simplified relation that takes into account the main parameters is given by [23]:

$$I_{SHG}(2\omega) \propto \left[\chi^{(2)} \frac{P}{\tau}(\omega)\right]^2 \tau \tag{20}$$

Where $\chi^{(2)}$ is the second order susceptibility of the material, *P* is the laser pulse energy, τ is the laser pulse width and ω is the laser pulse frequency. Based on this assumption at same laser average power condition, shorter is the laser pulse stronger is the SHG signal generated. Femtosecond laser sources generate SHG more efficiently than picosecond pulsed lasers, but this does not prevent the use of picosecond source for this technique as demonstrated in this work. SHG signal has a quadratic dependence with the excitation power:

$$I_{SHG}(2\omega, l) = \frac{2\omega^2 {\chi^{(2)}_{eff}}^2 l^2}{n_{2\omega} n_\omega^2 c^3 \epsilon_0} \left(\frac{\sin(\Delta k l/2)}{\Delta k l/2}\right)^2 I_{EX}^2(\omega) \tag{21}$$

Where l is the interaction length, $\chi_{eff}^{(2)}$ is the effective second order non-linear susceptivity, $n_{2\omega}$ and n_{ω} the refractive index of the material at the two frequencies and I_{EX} is the intensity of the excitation signal. SHG signal can be efficiently generated and propagated, if the wavevectors satisfy the phase matching condition $\Delta k = 0$:

$$\Delta k = k_{SHG} - 2k_{EX} \tag{22}$$

If the phase matching condition is not respected due to interference between generated signals there is an oscillation along the direction of propagation of the SHG intensity, with maxima in correspondence of odd multiples of l (the interaction length) and minima in correspondence of even multiples of l.

Laser sources for CARS microscopy

The excitation sources choice is a critical step in CARS microscopy design and depending on this choice different results can be achieved. There are several parameters that determine the characteristics of the excitation sources used for CARS microscopy. In many applications a commercial confocal microscope has been modified in a way to accept at its optical input a combination of optical beams that excite the Raman vibration of a chemical specie and thus the generation of the CARS signal from the specimen. In the first applications of CARS microscopy visible pulsed laser with a pulse length of few picoseconds have been used [24], this choice has led to a strong non-resonant background signal that limited the sensitivity of the instrument. Subsequent modifications have involved the use of near infrared sources that showed better performance in terms of reducing non-resonant signal of solvent.

The continuous evolution of the excitation sources has also led to an evolution of CARS microscopy techniques, the use of femtosecond lasers, optical parametric oscillators (OPO) or photonic crystals fiber (PCF) opened new roads on the possibility of tuning wavelengths on a wide range and implement several CARS micro-spectroscopy techniques.

Two picosecond dye-lasers pumped by a mode-locked argon laser

In the first work on CARS microscopy [24] the sources which were used were based on two dye lasers synchronously pumped by a continuous argon laser. One of the two laser was based on the fluorescent rhodamine 6G molecule and generated a pulse of 6 ps, that could be tuned in a range between 565 nm and 620 nm with a repetition rate of 80 MHz and an average output power of about 250 mW. Another dye laser that generated the Stokes pulses was based on the fluorescent molecule 4-(dicyanomethylene)-2-methyl-6-(para-dimethylaminostyril)-4H-pyran and generated a pulse of 8 ps, that could be tuned to a range of between 620 and 700 nm and an average output power of 150 mW.

In this set-up, it was not easy to overlap and align the two dye lasers to realize the phase matching condition necessary to the generation of the non-linear optical CARS process. A huge disadvantage of these laser sources was their emission in the visible region that significantly increased the non-resonant contributions, overwhelming the resonant CARS signal when the concentration of the analyte was not high enough.

A femtosecond laser with an optical parametric amplifier (OPA)

In the work in which CARS microscopy was brought again to the attention of the scientific community [25] with the capability to obtain also a three-dimensional imaging of the sample, some of the limits of the Duncan's group work [24] have been overcame, the exciting sources have been obtained through a

regenerative amplifier in Ti: sapphire (Rega model by Coherent) that was pumping an optical parametric amplifier (OPA). This system also needed a continuous laser pump of few watts of power, using a system based on argon or on a duplicated Nd:Vanadate. In this case, the regenerative amplifier serves to generate ultra-fast pulses, which can have a length ranging from few femtoseconds to few picoseconds depending on how the system is conceived. Typically the regenerative amplifier consists in a cavity in where are placed an amplifying optical crystal and some optical switching devices like acousto-optic modulator (AOM) or electro-optical modulator (EOM) and polarizers.

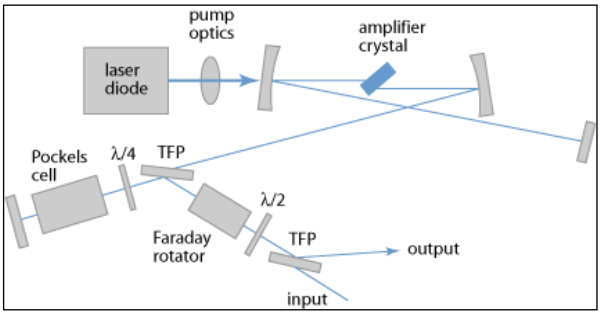

Fig. 2.6 Optical scheme of a regenerative amplifier.

The operating principle of the regenerative amplifier can be described with the following basic steps:

- The laser pumps the amplifier crystal inside cavity accumulating energy.
- The laser beam inside the cavity is modulated through the modulator (AOM or EOM) to create a pulse of duration less than the cavity round-trip.
- At this point the impulse is continually amplified in each round-trip crossing the amplifier crystal that increases its efficiency just when the optical power exceeds a certain threshold.
- After a certain number of passages in the cavity the gain saturates and the regenerative amplifier stabilizes generating ultrafast pulses at the output that can be further compressed in a later stage.

If the amplifier crystal used is made in Ti: sapphire, the wavelength of the output pulse will be in a range between 650 and 1100 nm, generally around a value close to 800 nm. Regenerative amplifier output can be used as pump pulse for CARS microscopy and partly used as pump for optical parametric amplifier (OPA). Optical parametric amplifier is based on the properties of some crystals that have a lack on the inversion symmetry and that are characterized with a non-linear second order susceptibility $\chi^{(2)}$ [26].

In these crystals an incident pump laser generates a sum of two optical beams, the so called signal and idler that have longer wavelengths, in a way that the sum of their relative energies is equal to that of the pump laser photon. Since that the pump laser energy is completely converted in the crystal while generating signal and idler beams, there are not heating phenomena. This non-linear optical process is sensitive to the condition of overlapping phase (phase matching), which is obtained by placing the crystal in a certain angle of incidence with respect to the pump laser. Changing the crystal temperature it is possible to change its susceptibility and thus the wavelengths of the emitted beams, allowing a wavelength tuning on a specified range according to the system.

Using ultrafast pulses to pump the optical parametric amplifier, also generated beams are pulsed, although generally with a longer duration due to the dispersion addition by optical parametric amplifier lenses. Even in this case it is possible to compress the pulse with an additional stage. Stokes signal can be obtained using the OPA output as for example in the work of Zumbusch et al. where it could be tuned on a range between

1.1 and 1.2 μm [25]. This type of source has the disadvantage of requiring expensive and even complicated optical systems that requires also continuous maintenance and characterization to verify periodically the stability of optical parameters.

Two synchronized mode-locked lasers

One of the first techniques used to generate infrared pump and Stokes pulses with a large tuning range of Raman bands excitation (between 500 and 3500 cm^{-1}), was obtained using two Ti: sapphire mode-locked picosecond laser systems, synced together via a feedback system [27,28].

This system presents a high spectral resolution (~2 cm^{-1}) using pulses of ~3 ps, but it has also some drawbacks like for example the presence of a time jitter between the two generated pulses that limits performance. Moreover, the two generated pulses must be aligned to overlap perfectly in time and space.

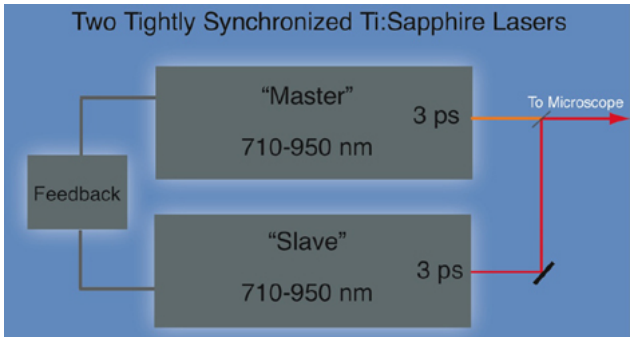

Fig. 2.7 Scheme of two mode-locked synchronized lasers.

An optical parametric oscillator (OPO) synchronously pumped by a frequency doubled Nd:Vanadate picosecond laser

An alternative source is an optical parametric oscillator (OPO) pumped by a frequency doubled in Nd:Vanadate picosecond lasers with two outputs one peaked at 1064 nm the other at 532 nm.

An optical parametric oscillator is a source that generates a radiation similar to that of a laser, but uses a parametric amplification through a nonlinear crystal instead of a stimulated emission. It can therefore be considered a cross between a laser and an optical parametric amplifier:

- As in a laser there is a resonant cavity;
- As an optical parametric amplifier there is a nonlinear crystal that generates and amplifies signal and idler optical beams at wavelengths different than that of the pump.

The main characteristic of an optical parametric oscillator is the chance to obtain wavelengths that are difficult to obtain with lasers with large ranges of tunability that can cover several hundreds nanometres.

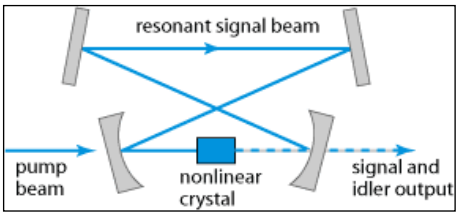

Fig. 2.8 Optical scheme of an OPO internal cavity.

The pump laser power must exceed the nonlinear crystal threshold power in order to make it works properly. This is easily achievable using a pulsed pump lasers, which condenses high optical power into a short time. Again to get the signal and idler beams generation it must be realized the phase matching condition. The way the phase matching condition is obtained determines the output wavelength that can be varied by changing the temperature of the crystal, the angle of incidence or finely adjusted by changing the length of the resonant cavity.

To obtain a synchronism between the pump and the impulse generated by the OPO, the cavity length must be adjusted in such way that the passage frequency of the pulse along the crystal is equal to the repetition rate of the pump laser. The duration of the pulse at the OPO output is generally comparable to that of the pump and sometimes under certain conditions, when there is a significant decoupling of group velocity, can be even shorter [29].

If signal and idler are used as excitation sources for CARS microscopy, picoseconds pulses allow obtaining a good spectral resolution (about 5 cm^{-1}). The OPO output beams can be tuned over a wide range of wavelengths (from 690 to 2300 nm) allowing a possible excitation range of Raman vibrations between about 500 and 5000 cm^{-1}.

With this system it is also possible to exploit the signal and idler exiting from the same OPO output. This configuration allows having the two signals already overlapped in time and in space, ready to be focused using the microscope on the sample. Both pump and Stokes pulses are generated from the same pump laser avoiding time jitters between the two signals.

Femtosecond laser with photonic crystal fiber (PCF)

Combining a femtosecond laser with a photonic crystal fiber it can be obtained a very extensive optical spectrum through the generation of so-called supercontinuum. Using for example the output of a Ti:sapphire femtosecond laser peaked around 820 nm as pump for CARS microscopy and the generated supercontinuum as a broadband pulse of Stokes, it is possible to realize a multiplex CARS over a large Raman spectrum [30].

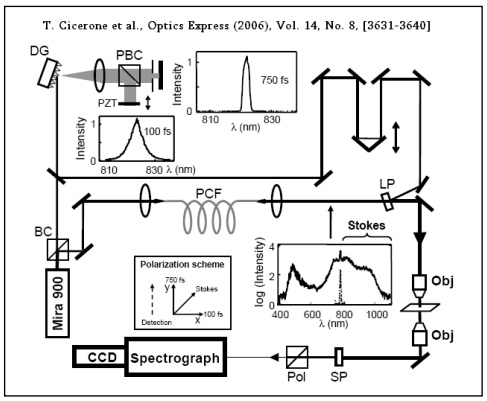

Fig. 2.9 Optical scheme of multiplex CARS system based on a PCF fiber.

This configuration avoids the time jitter by using the same source for both the pump and Stokes pulses, but it has however the disadvantage of having different beams to focus and align so that the impulses are spatially and temporally overlapped.

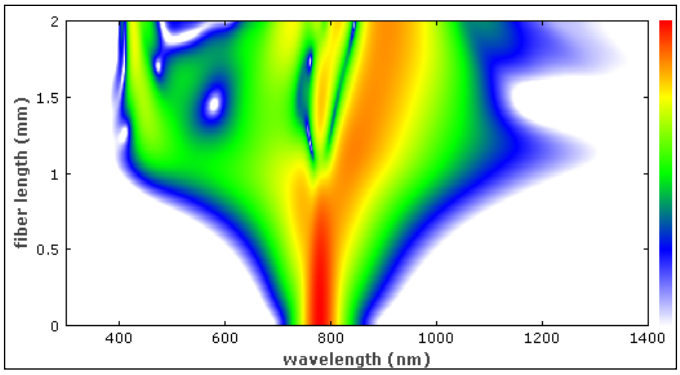

Fig. 2.10 PCF fiber supercontinuum generation in function of its length.

Main implementation techniques developed for CARS microscopy

In this section are discussed briefly the main techniques that were implemented in order to realize CARS microscopy and to reduce the inherent non-resonant background, which in certain applications could limit the performance of the microscope.

Forward detection CARS (F-CARS)

This is the technique that has been used since the early published works and as the name suggests, CARS signal is measured in the direction of propagation of the pump and stokes lasers. The two pump and stokes lasers are overlapped in time and space and focused on the sample with a high numerical aperture objective easing the necessary phase matching condition for the CARS signal generation.

Using an objective with a large numerical aperture the pump and stokes laser beams interact with the sample with many angles of propagation through the wide wave vectors cone and the little interaction length [25]. Moreover large objective numerical aperture restricts the excitation of the sample to a small volume, allowing a non-resonant noise reduction, fewer damages on the specimens and the chance to image the sample in three dimensions [25].

The CARS signal is filtered to remove the excitation source components and detected after the sample in the direction of propagation. Using a set of galvanometric mirrors it is possible to scan the lasers on the sample and reconstructing the image pixel by pixel. The signal obtained is typically very intense, but unfortunately this configuration has the disadvantage to generate also a strong non-resonant background signal due to the solvent, which limits the sensitivity when are observed very small objects with sizes comparable to the incident lasers wavelengths, as it was described in the previous chapter.

The non-resonant background noise is generally caused by non-resonant electronic transitions related to the contributions of the third order susceptibility $\chi^{(3)}$ [31], to reduce the probability of generating electronic transitions which are higher using lasers in the visible region [24], it is better to use instead near infrared lasers [25]. Moreover longer wavelengths minimize Rayleigh scattering phenomena in heterogeneous samples, allowing a deeper penetration into tissues that is desirable in many applications [25]. To use F-CARS the sample should not be too opaque seen that the generated CARS signal generated must traverse all the thickness of the sample, with consequent attenuation of its intensity.

Epi-detection CARS (E-CARS)

In order to reduce the non-resonant background noise radiation it was evaluated the possibility to detect the CARS signal that propagates in the opposite direction to that of the excitation lasers (epi-detection, E-CARS). The CARS signal is collected through the same large numerical aperture lens used to excite the sample. A dichroic mirror is used to deflect the excitation wavelengths and to transmit the CARS signal generated in the sample that can be detected by a photomultiplier tube.

In this case the obtained CARS signal is less intense than that obtained in forward direction, but offers the possibility to better image smaller objects with a size comparable to the excitation wavelength [8].

This implies that if the excitation volume is kept very small by using a large numerical aperture objective, the contribution due to the solvent (with a larger size than the excitation wavelengths) is significantly reduced compared to the F-CARS [8]. For objects larger than the excitation wavelengths is still a good idea to use the F-CARS in addition to the E-CARS technique in order to get benefits from both techniques.

For highly opaque E-CARS technique could result in more intense signals than those obtained using the F-CARS one.

Polarization sensitive CARS (P-CARS)

A method of reducing almost totally the non-resonant noise was developed using the difference in polarization between the resonant and non-resonant CARS signal [32]. Already in the 70s had been demonstrated the possibility of CARS spectroscopy using polarizers [33].

The polarizers are placed either after the pump and stokes laser sources, either before the CARS signal detector. The pump laser is polarized linearly along the x-axis and the Stokes laser is polarized linearly with an angle ϕ with respect to the x-axis as in figure 2.11.

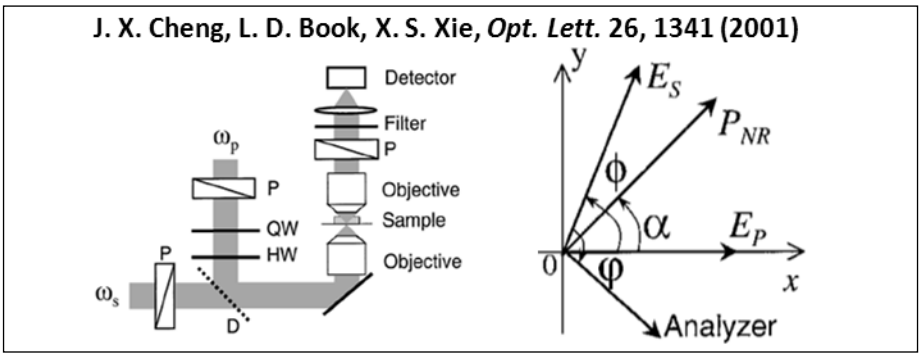

Fig. 2.11 Optical scheme with polarizers and phase diagram.

The optimal angle α which eliminates completely the non-resonant signal maximizing the resonant CARS signal must be equal to 45° [32]. The relationship that links the angle ϕ with the angle α is given by:

$$\phi = \tan^{-1}(3\tan\alpha) \tag{23}$$

thus the angle ϕ which eliminates completely the non-resonant signal is equal to about 71,6° [32].

In Figure 2.11 it is also shown the simplified optical scheme for this technique. A quarter-wave plate and an half-wave plate, introducing a phase shift of 135° placed along the path on the polarized pump beam to compensate for the phase distortion introduced by the dichroic mirror used for align collinearly the polarized pump and stokes beams [32].

With this technique the resulting CARS intensity is lower than that obtained with a classic F-CARS set-up without using polarizers, but the non-resonant noise can be reduced almost completely both for the solvent and the objects to image in the sample.

Time Resolved CARS (T-CARS)

Another way to discriminate better the resonant CARS signal eliminating almost completely the non-resonant background noise can be realized introducing a delay between the first and second pump pulse, the latter also called probe pulse. The principle of this method is based on the decay of the Raman molecular vibration (RFID – Raman free induction decay). Free decay time of Raman molecular vibration is a specific parameter of the Raman resonant transitions that strongly depends on molecule and that could also be used to obtain a time-domain spectroscopy [34].

Introducing a delay between the two almost simultaneous pump and stokes pulses and the probe pulse it is possible to perform a time domain spectroscopy which could reduce strongly the non-resonant signal

coming from the solvent or by other molecules present in the focal volume. Decay time of resonant transitions is typically longer than those generated from other non-resonant transitions. When the probe pulse interacts with the sample after a certain imposed delay, only the molecules in resonant excited state could contribute to the CARS signal generation.

This technique is suitable in those systems that use laser pulses having duration of a few hundred fs or less, as decay times can be very short. Moreover pulses of short duration can be obtained a better temporal resolution to characterise the target molecules decay times. It is not excluded a priori that pulses with duration of some picoseconds the system could give good results, but shorter is the momentum lower is the smallest delay that could be introduced, facilitating the use of this technique in those cases with very fast decays.

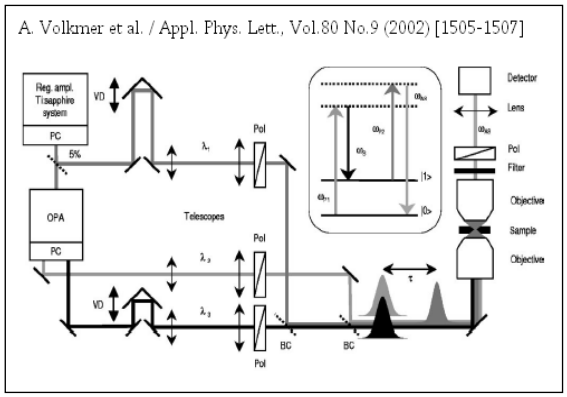

Fig. 2.12 Optical scheme of a T-CARS system.

The delay can be introduced with a delay line extending the optical path of a portion of the pump laser signal. The propagation delay of the probe pulse is directly linked to added path length that can be changed independently using for example automated high-precision piezoelectric actuators.

Interferometric CARS (I-CARS)

As it was already enounced, one of the biggest complications of CARS microscopy is the presence of the non-resonant background signal that could even delete the CARS signal when the resonant analyte concentration is low or the Raman band to be analysed is inherently weak.

Interferometric technique reduces strongly the non-resonant signal without attenuating the CARS signal intensity. The classic excitation signal defined as $E_{EX} = E_p^2 E_s$ is mixed with a well-controlled reference signal, called local oscillator E_{LO}, that has the same wavelength of the expected CARS signal. The total CARS signal can be written as [35]:

$$S = |E_{LO}|^2 + |E_{as}|^2 + 2E_{LO}E_{EX}\left\{\left[\chi_{NR}^{(3)} + \Re\left(\chi_R^{(3)}\right)\right]\cos\phi + \Im\left(\chi_R^{(3)}\right)\sin\phi\right\} \qquad (24)$$

Where ϕ is the phase difference between the CARS signal and the local oscillator. The last two terms of the equation refer to interferometric mixing. If ϕ values 90°, the contributions due to the imaginary resonant will be maximized while the contribution due to the non-resonant will vanish completely. If instead, ϕ values 0° only the real part of the signal is detected.

Revealing the imaginary part of the terms relating to the interference with the local oscillator, the background signal is suppressed; moreover with this technique the interference term of the CARS signal varies linearly with the concentration of molecules related to the selected Raman band.

A possible implementation of this technique is described in literature using a Mach-Zehnder interferometer [35].

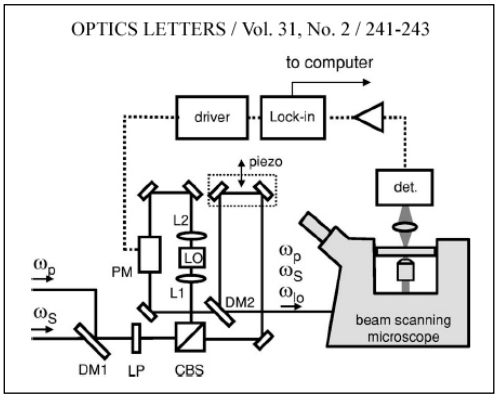

Fig. 2.13 Optical scheme of an I-CARS system based on a Mach-Zehnder interferometer.

Stokes and pump signals are collimated and sent within the Interferometer, one of the two arms contains a cell of d-DMSO (dimethyl sulfoxide deuterated) to generate a strong non-resonant signal at the anti-Stokes frequency, obtaining the local oscillator (LO in Figure 2.13). A phase modulator (PM in Figure 2.13) modulates at 10 MHz to about 10° the phase of the local oscillator. In the other arm a pair of mirrors mounted on a piezo actuator finely adjusts the difference in optical path length between the two arms. The modulated local oscillator beam is then aligned with the pump and Stokes pulses and thus sent together in the microscope and then on the specimen.

M. Jurna et al., Vol. 15, No. 23 / OPTICS EXPRESS 15207

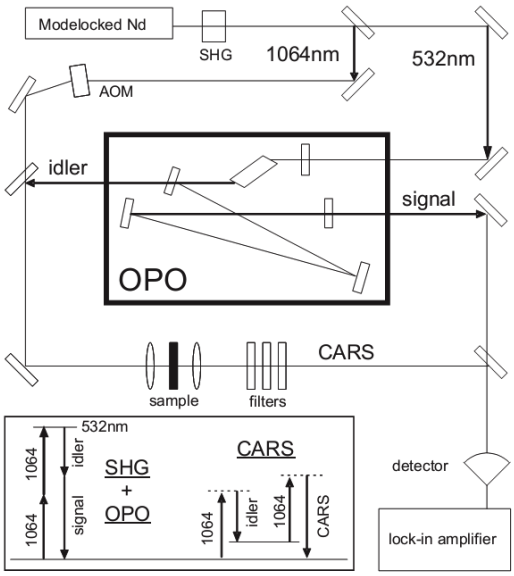

Fig. 2.14 Optical chain for the phase-preserved generation of wavelengths for the CARS process. The inset shows the energy diagram for both paths to the CARS wavelength.

The CARS signal generated in the sample is directly mixed with the local oscillator and the phase modulation of the latter becomes an amplitude modulation of the CARS signal. The signal is revealed through a photomultiplier tube and sent to a lock-in amplifier to isolate the heterodyne signal that corresponds to the interference term of eq. (24).

Changing the phase between the local oscillator and the CARS signal it is possible to have contrast for $\mathrm{Im}\,\chi_R^{(3)}$ eliminating completely the contribution due to the non-resonant signal component. With this technique the CARS signal can be amplified thanks to the interference with the local oscillator only acting on the local oscillator power without changing the incident pump and Stokes pulse power.

Another interesting implementation of this technique coupled has been implemented using as local oscillator the OPO signal output and as excitation scheme the OPO idler with the 1064 nm output of the OPO pump laser [36, 37]. This scheme is particularly advantageous because it is possible to obtain a noise-free amplification, jitter-free operation and wavelength scanning without synchronization errors using excitation sources that are generated by the same pump laser.

Multiplex CARS (M-CARS)

The technique called multiplex CARS allows to obtain a Raman Spectroscopy of a sample exciting a series of Raman bands broader than what it would be obtained using a narrow band CARS microscope with pulse length of few picosecond for pump and stokes. It has been shown that pulses with a duration of a few picosecond lead an higher ratio between the resonant and the non-resonant CARS signal strengths than that obtained using shorter femtoseconds pulses [25]. Picosecond pulses have a spectral width comparable with the typical peaks of the Raman bands (~2 cm^{-1}) and thus the power of the pump and Stokes pulses is used with high efficiency to generate the CARS signal [38].

If Stokes pulses with duration of some tens of femtoseconds (150 cm^{-1}) and pump pulses with duration of few picoseconds (~ 2 cm^{-1}) are used, a wider Raman spectral band can be excited and a CARS signal with a wider bandwidth can be generated and thus decomposed using a spectrometer.

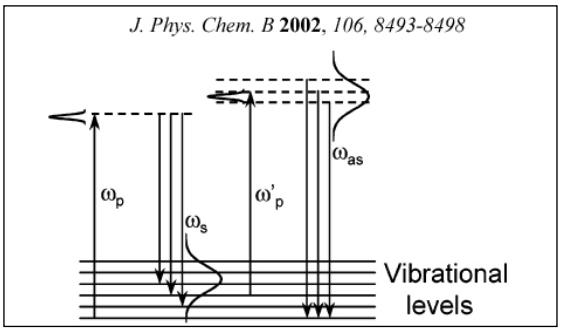

Fig. 2.15 Energy bands diagram related to the pump and Stokes pulses, in which femtosecond pulse is employed for the Stokes signal.

In this way it is possible to obtain a fast spectroscopy on a bigger part of the Raman spectrum simply tuning the wavelengths and the pulse lengths of the pump and Stokes lasers.

This technique coupled with a high numerical aperture lenses microscope makes it possible to rapidly characterize extremely small volumes from the chemical point of view, allowing a 3D characterization of the samples. It has also been demonstrated a technique to increase the contrast of the resonant CARS signal by integrating M-CARS with P-CARS [38].

The limiting factor of this technique is the requirement of an ultrafast and sensitive spectrometer that allows fast acquisition of spectra for each pixel of the image. Moreover this technique requires also a motorized XY microscope stage, instead of scanning galvanometric mirrors to ensure a perfect alignment of the CARS beam with the spectrometer optics.

Important properties and parameters to be measured in regenerative medicine applications

Regenerative medicine and tissue engineering are some of the most promising biomedical technologies and their aim is to provide custom-made medical solutions for injured or diseased patients. The common idea of these two technologies is to regenerate a whole or part of a tissue or of an organ to be implanted into the patient. These technologies to be developed, need multidisciplinary teams because are very complex and are based on several processes that involve a deep study at each level, from the cell biology, to the structural and material composition of the scaffolds, from the cells harvesting to the surgical implantations.

In this field it is very important to study the interactions between cells and extracellular matrix (ECM), the stem cells differentiation, the growth factors, the scaffolds used in the cell cultures, the bioreactors for cell cultures and the validation methods for the final clinical use.

Each of these aspects needs specific measurement capabilities to verify the progress of the cell culture and the quality of the tissue. In general it is very important to analyse cells viability and proliferation of the cultures, because these are the two important indexes of how the cells are growing.

When it is studied the cells-ECM interaction, generally the most important parameters analysed are related to the cell adhesion, the cell migration, the cell shape, the chemical composition of the ECM, the tissue organization and the cellular signalling.

The stem cells differentiation is very important in regenerative medicine because in many products, stem cells are used as culture cell type that later differentiates in the specific types requested for the final tissue. Differentiation process could be analysed to know what type of cells are present in culture, when cells started to differentiate, their spatial distribution, etc. Moreover these analyses allow characterizing also the functionality of the growing factors that are used also to stimulate chemically the differentiation process.

Investigating the structural and topographic properties of the scaffolds used in regenerative medicine is also very important because, as it has demonstrated in several studies [39-50], the scaffolds characteristics like chemical composition, topographic features, and mechanical properties like stiffness, strength, and permeability influence cells growing and tissue quality.
The use of bioreactors that provides also automation and user-independence, allows supplying stimuli to the cell cultures, monitoring and controlling with real-time feedback cells growing during the incubation. These tools need to sense a large number of physical, chemical and biological parameters like the temperature, the pH, the dissolved oxygen and carbon dioxide chemical contaminants, the concentration of significant metabolites/catabolites and the sterility of the system.

Many traditional techniques used to measure these parameters are destructive and/or invasive, require manipulation of the cells and do not provide spatial information. Gene expression measurements that are widely used to perform genetic and proteomic analysis of the sample in order to determine for example, the cell types or the proteins expressed, contemplates destructive steps and loosing of the spatial distribution of the proteins. Western blot protein analysis needs to destroy samples and requires a consistent amount of protein to have accurate results. Many immunofluorescence techniques for protein imaging give information on the spatial distribution of the protein but samples need to be fixed and/or sectioned. Cytofluorimetry used for cell counting and sorting needs sample manipulation to detach cells from scaffolds.

Scaffolds can be characterized using different measurement techniques. For instance, in scaffold morphological characterization, usually properties related to pore-solid distributions are measured, evaluating size, geometry and interconnectivity of the pores and the void-space ratio. Generally these properties are evaluated through imaging techniques [51] based on x-ray micro-tomography (micro CT) [52-54], scanning electron microscopy (SEM) [55, 56] and through permeation of fluids [57-59], or atomic force microscopy (AFM) when nanostructure properties of the scaffold surface are analysed [60]. Characterization of scaffolds from its biological behaviour is also relevant [61] and usually it is done evaluating the cytotoxicity, the cell adhesion, proliferation, differentiation, mobility and migration, using several techniques like optical microscopy, laser scanning confocal microscopy, fluorescence, absorbance, gene expression, etc. [62-66].

The micro CT technique is widely used for scaffold characterization and although it has important advantages like high spatial resolution together with high material penetration, which allow three-dimensional samples reconstruction, it makes use of an x-ray source that could be harmful for living samples. SEM makes use of an electron beam that does not allow analysing living samples and it could need also specific sample preparation. Moreover SEM does not allow three-dimensional reconstruction of the sample.

Multimodal CARS-SHG microscopy could overcome some of these limitations offering the advantages to image 3D living samples without the need of staining procedures or samples manipulations.

3. Experimental setup of the multimodal CARS-SHG-TPEF microscope developed at INRIM

Coherent anti-Stokes Raman scattering can be generated when two laser sources are used as excitation signals (pump and Stokes beams), that have an emission wavelength difference that can be tuned to the active Raman vibrational transition of the chemical species to be observed in the sample. A CARS microscope can be realized using a commercial laser scanning microscope that focuses the excitation radiations onto the sample and to collect the generated CARS radiation. A dichroic mirror must be used in order to separate the excitation beams from the CARS light. The microscope scans the excitation sources on the sample and using a specific software an image of the Raman active sites of the sample is built, allowing precise localisation of the chemical species under study.

For biological imaging purposes, near infrared laser sources are the best choice, because in that spectral region absorption of radiation and subsequent heating/damage of the biological samples is minimised.

Moreover, biological material mainly consist of proteins and lipids, which show marked Raman features in the region around 2800-3000 cm^{-1}, due to the C-H bond stretching vibration transitions, and in the so called fingerprint region around 500-1800 cm^{-1}. These spectral regions should be therefore accessible to the tuneable laser source. Moreover, source lasers operating in pulsed regime are advantageous since very strong peak power can be reached with moderate average powers. However, in order to maintain a certain spectral resolution capability, the pulse duration cannot be too short. Pulses in the picosecond regime offer a very good trade-off in terms of achievable spectral resolution and obtained peak powers at average powers not dangerous to biological materials.

According to these criteria, the configuration based on an optical parametric oscillator (OPO) pumped by a frequency doubled in Nd:Vanadate picosecond lasers with two outputs, one centred at 1064 nm the other at 532 nm, was chosen. A passively mode-locked Nd:YVO_4 (Yttrium Vanadate crystal doped with Neodymium) laser emitting at 1064 nm was acquired as a master source (HighQ Picotrain). This optical source emits a continuous train of 10 ps pulses at the repetition rate of 76 MHz. The Nd:YVO_4 laser is equipped with a second harmonic generation (SHG) unit which doubles with high efficiency the frequency of the Nd:YVO_4 oscillator. The 532 nm output of the SHG unit, based on a nonlinear Lithium-Triborate (LBO, LiB_3O_5) crystal is used to synchronously pump an OPO which is the second source that has been acquired (APE Levante Emerald). The OPO acts as the tuneable source. The OPO uses a non-linear LBO crystal as a parametric amplifier in a doubly resonant optical cavity. Tuning is achieved by changing the operation temperature of the LBO crystal. The thermally induced change in refractive index changes the phase matching condition and consequently the two emission wavelengths of the OPO. The tuning range is about 690-1040 nm for the signal wave and about 1100-2200 nm for the idler wave.

The pump laser has two output ports, one for the 1064 nm radiation and the other for the green radiation. The power exiting the two ports can be adjusted electronically. The full-blown output at 1064 nm is around 10 W, in this configuration the 532 nm output is minimum. The maximum output at 532 nm is around 5 W, with about 100 mW of radiation exiting the 1064 nm port.

The OPO output can be mechanically set in two configurations:

1) Signal and idler both exiting the same port;
2) Signal and idler exiting separate ports.

The possibility of combining the signal or idler radiation separately with that at 1064 nm adds certain flexibility in the implementation of the excitation schemes for the CARS interaction. This fact has been exploited in the design of the experiment described below.

Since the first goal of the activity was that of observing a CARS spectrum on a homogeneous sample, the forward scheme has been adopted. Polystyrene has been chosen as a reference material to be observed. The Raman spectrum of polystyrene is well known and shows strong features in the region around 3000 cm^{-1}: a strong peak at 3060 cm^{-1} and a series of secondary peaks in the region between 2800 cm^{-1} and 3000 cm^{-1}, which can be reached with the sources available in the laboratory. The vibrational spectrum of the polystyrene sample used in the CARS experiments was previously characterized using a linear Raman micro-spectrometer (InVia RE02 by Renishaw). The measured spectrum is shown in Fig. 3.1.

The structure of polystyrene is shown in the inset of Fig. 3.1. The benzene rings are responsible for the Raman bands around 1000 cm^{-1} and 1620 cm^{-1}, to which stretching of the C-C bond also contributes. The bands around 2900 cm^{-1} are due to stretching of the CH_2 and CH_3 bonds, whereas the strong peak around 3060 cm^{-1} is due to stretching of the C-H bonds.

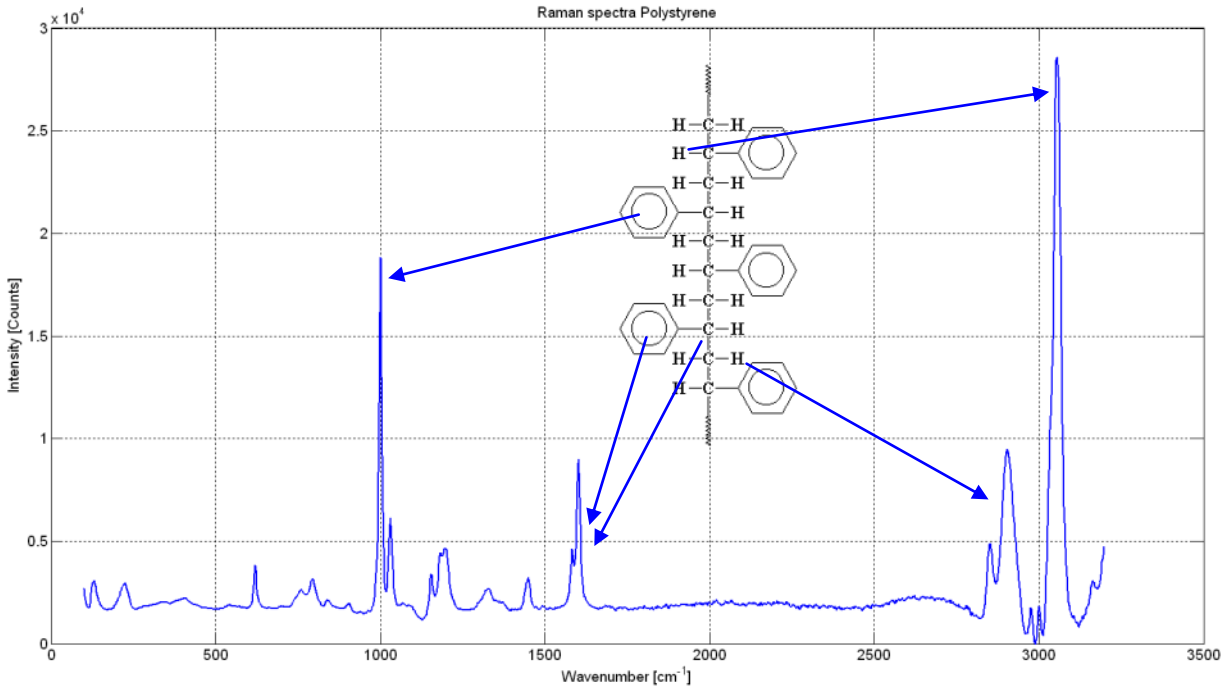

Fig. 3.1 Measured Raman spectrum of the Polystyrene plate used for the CARS experiments. Inset: Polystyrene structure and related Raman bands.

As a first step, in order to better understand the main experimental criticalities of CARS generation it has been decided to simplify the set up as much as possible in order to maintain strict control of the

experimental conditions. To this aim, for the initial CARS experiments the use of the confocal microscope, with its complex optics of which little is known in detail, has been avoided.

Signal-idler Excitation Scheme

The simplest way to implement an excitation scheme for CARS experiment is that of using directly the two wavelengths generated by the OPO. In particular, the OPO signal beam, being at a shorter wavelength, is used as the pump wave, whereas the idler is used as a Stokes wave. The relation between the emitted wavelengths and their frequency separation in cm^{-1} is shown in Fig. 3.2, together with the resulting CARS wavelengths. As it can be seen, in order to excite Raman transitions in the 3000 cm^{-1} region, the OPO signal wavelength should be set around 915 nm. The idler wavelength is around 1270 nm and the CARS signal is expected in the visible at a wavelength around 715 nm.

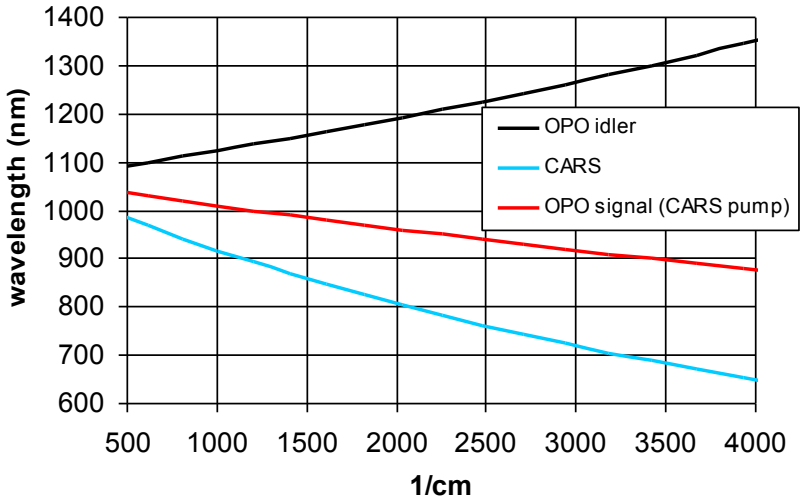

Fig. 3.2 OPO signal and idler wavelengths as a function of frequency detuning in cm^{-1}. Signal is used as a pump wave; the idler provides the Stokes wave. The expected CARS wavelength is shown as the cyan curve.

The main advantage of this scheme is that the signal and Stokes beam are already overlapped in space and time, as generated by the parametric oscillation synchronously driven by the pump pulses in the doubly resonant OPO cavity. The second advantage is that all the pump laser power can be used to pump the OPO, thus allowing very high CARS excitation powers to be achieved (total powers as high as 2.5 W with 5 W of 532 nm radiation at the OPO output ports). On the other side, the wavelength separation is rather large (about 350 nm). This feature may turn out in a drawback if the optics used for beam conditioning, focussing and collection is not optimised for NIR operation.

The schematic of the experimental set-up used for the implementation of signal-idler excitation scheme is shown in Fig. 3.3. The two combined beams exiting the OPO are brought to focus on the sample by a 10x microscope objective. The objective is mounted on a xyz translation stage to allow optical alignment with the collection optics and finely adjust focus on the sample. The collection optics consists of a 4x microscope objective mounted on a xyz translation stage, less precise than that of the launching optics. Both objectives are placed on mounts with tilt controls in the vertical and horizontal directions.

After the collection optics a filtering block is placed, to reject the pump and stokes wave and let the CARS radiation to reach the detector stage undisturbed.

The key element of the filtering block is the dichroic mirror DM740 that was chosen as excitation dichroic mirror of the microscope scan head, which separates the excitation signals from the CARS signal to be detected.

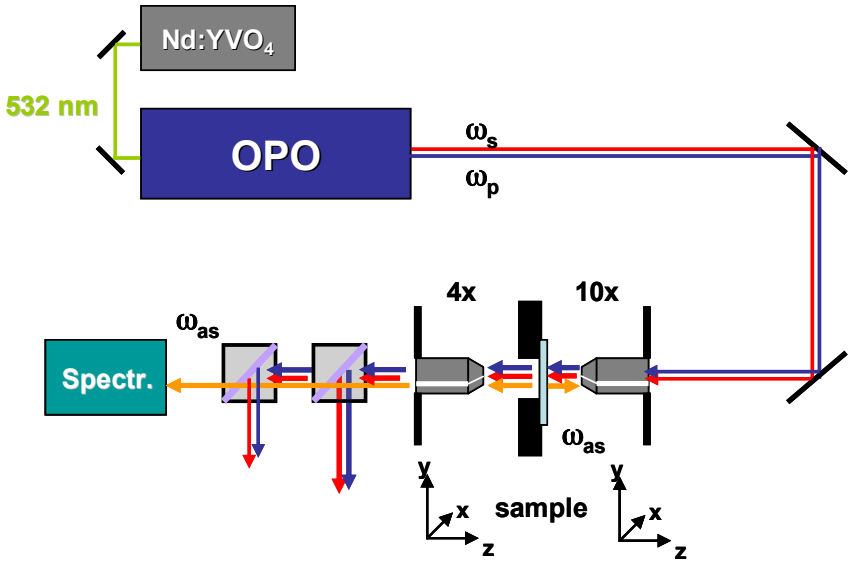

Fig. 3.3 Experimental set-up of the signal-idler excitation scheme.

The dichroic mirror has been therefore carefully characterised. Its spectral transmittance is shown in Fig. 3.5, as measured with a white lamp and a spectrometer in the visible-NIR (Avantes Avaspec 2048); the experimental set up is shown in the inset of Fig. 3.4. This dichroic mirror has been used in front of the detector to filter out the excitation beams. The filter exhibits a cut-off wavelength around 750 nm. The pump beam at 915 nm is well reflected. The behaviour at the idler wavelength (around 1270 nm) is not shown, because the used spectrometer is optimised for operation in the visible part of the optical spectrum and cannot detect light with wavelength greater than 980 nm. A characterisation carried out with an Optical Spectrum Analyser (OSA, Agilent 86146B) operating in the NIR shows that at 1270 nm the dichroic mirror acts approximately as a beam splitter with a reflectivity around 30%. It appears clearly that the CARS signal at 720 nm is just at the superior limit of the filter transmission, where the dichroic mirror transmittance starts deteriorating.

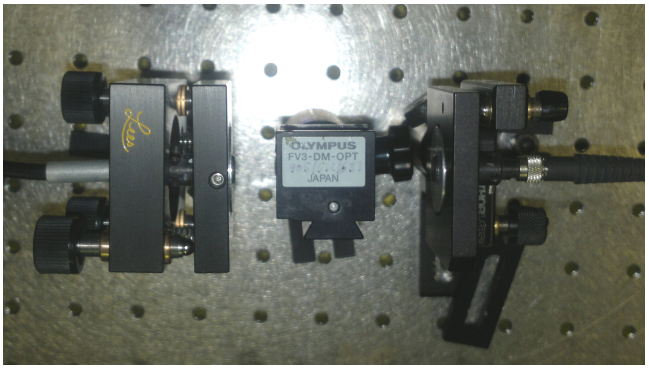

Fig. 3.4 Experimental set-up for spectral transmittance characterization of the optical components used.

The limitations set by the available dichroic mirror used as a filter in this configuration are shown in Fig. 3.7, where the wavenumber region over which CARS can be observed has been superimposed to the chart of Fig. 3.2. As can be seen the set up cannot explore spectral regions below 2950 cm^{-1}. Idler is only slightly